

AD-A084 387

BDM CORP MONTEREY CA

F/G 4/1

AN AIRCRAFT STUDY OF TURBULENCE DISSIPATION AND TEMPERATURE STR--ETC(U)

MAR 80 C W FAIRALL

N00014-78-C-0204

UNCLASSIFIED

BDM/N-004-80

NL

| 14 |
AD *
JUN 1987

June

June

END
DATE
ENTERED
6 80
DTIC

LEVEL

12

5

AU84387



DTIC
SELECTED
MAY 7 1980

C

FILE COPY

... .. approved
... .. sale: the
... ..

80 4 7 160

416162

12



P. O. Box 2019
2600 Garden Rd.
Monterey, California 93940
Phone (408) 649-3880

DTIC
ELECTE
MAY 7 1980
S
C

11
17 Mar 1980

14
Report No. BDM/M-004-80

10
Prepared by: C. W. Fairall
Naval Postgraduate School
Monterey, California 93940

12) 34

15
Contract /N00014-78-C-0204

6

AN AIRCRAFT STUDY OF TURBULENCE DISSIPATION
AND TEMPERATURE STRUCTURE FUNCTION IN THE
UNSTABLE MARINE ATMOSPHERIC SURFACE LAYER,

Approved for Release by NSA on 05-08-2014 pursuant to E.O. 13526

410163

FOREWORD

This report was prepared under Work Order No. 086412 of Contract No. N00014-78-C-0204 in support of a U.S. Naval Postgraduate School research project sponsored by the Naval Air Systems Command, AIR 370, and Naval Avionics Center, Indianapolis. This report describes the results of the second stage analysis of aircraft measurements of micrometeorological parameters made at Panama City, Florida, in 1978. The first stage of analysis has been given in a previous report (Technical Report No. BDM/M-008-79). The work was done in cooperation with Dr. Ralph Markson and Mr. Jan Sedlacek of Airborne Research Associates and Drs. Ken Davidson and Gordon Schacher of the Naval Postgraduate School.

Accession For	
NTIS GRA&I	
DDC TAB	
Unannounced	
Justification <i>per file</i>	
By <i>J</i>	
Distribution/	
Availability Codes	
Dist	Avail and/or special
A	

TABLE OF CONTENTS

	<u>PAGE</u>
FOREWORD	iii
LIST OF FIGURES	vii
LIST OF TABLES	ix
ABSTRACT	xi
A. INTRODUCTION	1
B. THEORETICAL BACKGROUND	3
C. INSTRUMENTATION AND ANALYSIS	5
D. FLIGHT PATTERN	7
E. SURFACE LAYER SCALING PARAMETERS	9
F. LADDER PROFILES	11
G. SURFACE LAYER DIMENSIONLESS TURBULENCE RESULTS	11
H. DISCUSSION	21
REFERENCES	23
INITIAL DISTRIBUTION LIST	xiii

LIST OF FIGURES

<u>FIGURE NUMBER</u>		<u>PAGE</u>
1	C_N^2/C_T^2 vs Altitude	2
2	The Expected Effect of the Lower Isotropic Limit on the Turbulence Measurements as the Aircraft Nears the Sea Surface	8
3	Locations of the Ladder Profiles in the Vicinity of Panama City, Florida	12
4	Ladder Profile #4	13
5a	Ladder Profile #1	14
5b	Ladder Profile #19	15
6a	Dimensionless Dissipation Measurements as a Function of Dimensionless Atmospheric Stability	17
6b	Dimensionless Temperature Structure Function as a Function of Dimensionless Atmospheric Stability	18
7	Weighted Average of R vs Altitude Where R is the Ratio of the Measured Value of the Turbulence Quantity to That Value Expected From Eq. 7a or Eq. 7b	19
8	Fractional Random Error in Predictions of Turbulence Profiles Form Near Surface Measurements Using Eq. 8a and Eq. 9a	20

LIST OF TABLES

TABLE NUMBER

1

SURFACE LAYER SCALING PARAMETERS

PAGE

10

ABSTRACT

The dissipation rate of turbulent kinetic energy, ϵ , and the temperature structure function parameter, C_T^2 , have been measured over water from the near surface ($Z = 3\text{m}$) to the top of the boundary layer. The near surface values of ϵ and C_T^2 were used to calculate the velocity and temperature Monin-Obukhov scaling parameters, u_* and T_* . The unstable data were used to evaluate the feasibility of extrapolating the values of ϵ and C_T^2 as a function of height with empirical scaling formulae. The dissipation rate scaling formula of Wyngaard et al. (1971a) gave a very good fit to an average of the ϵ data for $Z < Z_i - 100$. Although the C_T^2 data obeyed a $Z^{-4/3}$ height dependence for $0.1 Z_i < Z < 0.5 Z_i$, the scaling formula of Wyngaard et al. (1971b) disagreed with the average C_T^2 by as much as 50%. At this point it is not clear if the discrepancy is a unique property of the marine boundary layer or if it is simply some unknown instrumental or analytic problem.

THE BDM CORPORATION

A. INTRODUCTION

This paper is a report on measurements of temperature structure parameter, C_T^2 , and rate of dissipation of turbulent kinetic energy, ϵ , made from a light aircraft using microthermal sensors as part of a study of turbulence in the marine boundary layer. A typical flight included measurements as low as three meters above the sea surface in an effort to characterize the surface layer turbulence parameters. The flights were usually extended well above the inversion - a maximum altitude of three kilometers being typical.

The data were gathered near Panama City, Florida, as part of a program of marine boundary layer research, the ultimate goal of which is the formulation of a model that will allow reasonable estimates of atmospheric turbulence and mean properties from the surface throughout the entire marine boundary layer and immediately above. Such a model would have application to such varied subjects as turbulent transport of heat, water vapor and pollutants, optical propagation, aerosols, radar propagation, and communications.

For example, C_T^2 is important for optical propagation studies due to its relation to the index of refraction structure parameter, C_N^2 , (Friehe, 1977),

$$C_N^2 = (79 \times 10^{-6} P/T^2)^2 (C_T^2 + .11 C_{TQ} + 3.2 \times 10^{-3} C_Q^2) \quad (1)$$

where C_Q^2 is the humidity structure parameter, C_{TQ} the cospectrum structure parameter, P is the pressure in mb, T the absolute temperature, and Q is in gm/m^3 . Overland the water vapor fluctuation contribution is usually negligible, so one can write

$$C_N^2 = (79 \times 10^{-6} P/T^2)^2 C_T^2 \quad (2)$$

This relationship is shown in Figure 1 with C_N^2/C_T^2 as a function of altitude for the U.S. Standard Atmosphere. In the marine boundary layer equation (2)

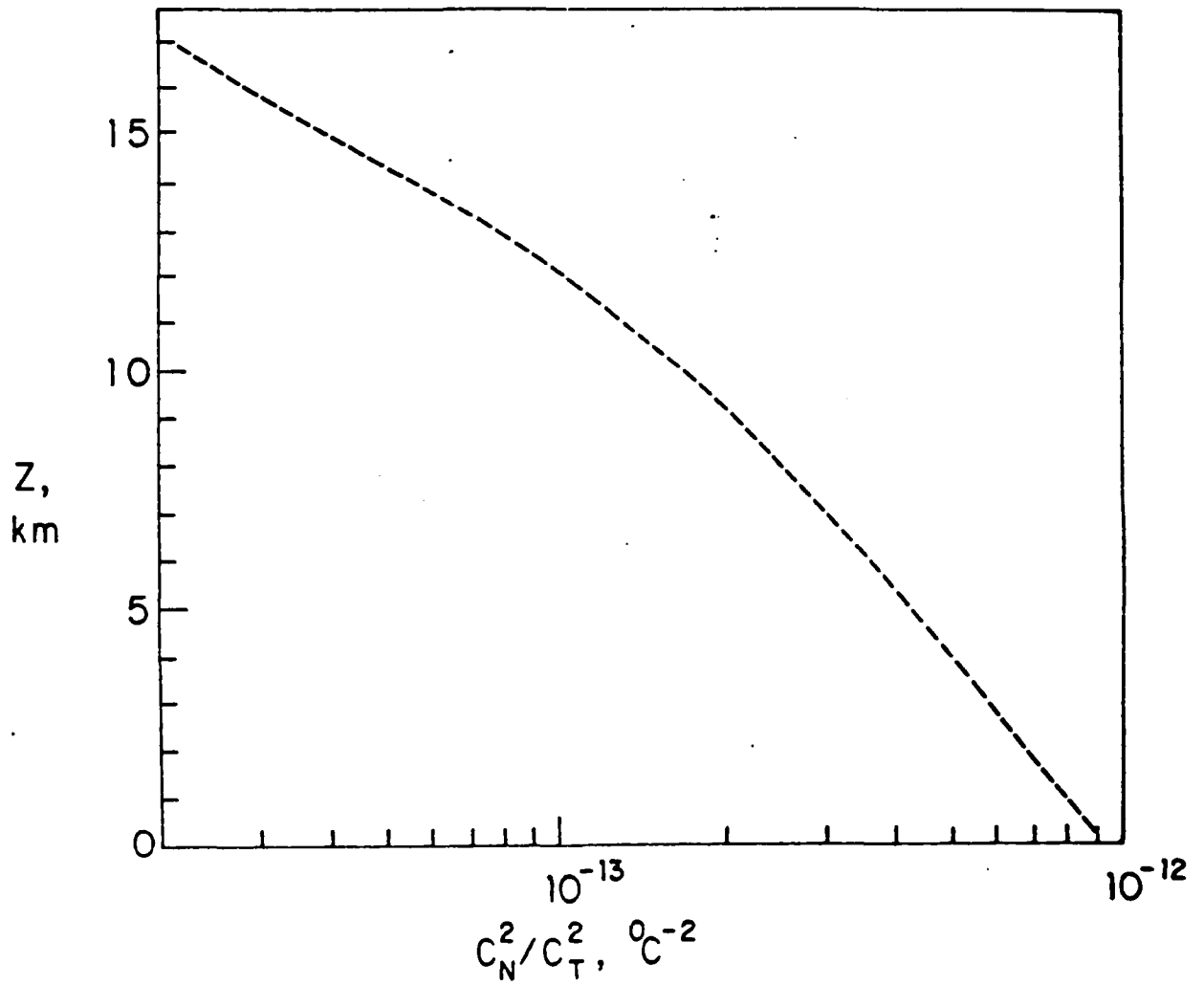


Figure 1. C_N^2/C_T^2 vs Altitude Based on Eq. 2 for the U.S. Standard Atmosphere

THE BDM CORPORATION

is only an approximation because of the large vertical water vapor fluxes that can be present over the ocean (Wesley, 1976). Friehe *et al.* (1975) found for the San Diego FLIP data that the C_T^2 contribution to C_N^2 was typically 70%. Ideally, one's model should be equally adept at handling temperature and water vapor height dependences.

This paper will focus on the utilization of the data to examine certain aspects of the Monin-Obukhov similarity (MOS) expressions for the dimensionless temperature structure function and the dimensionless dissipation function in the marine atmospheric surface layer. The validity of the existing empirical expressions of the asymptotic height dependences, variance of the data from surface extrapolations, and the influence of the height of the boundary layer will all be explored. Of the nine days on which flights were made, seven were characterized by unstable surface layers and two by stable surface layers. Since the height of the boundary layer was so low on the stable days (typically 100 meters), the influence of the height of the boundary layer tended to dominate the surface layer conditions causing most of the quantitative analyses mentioned immediately above to be of dubious relevance. In view of this, the analysis of the surface layer scaling properties was restricted to the unstable data.

B. THEORETICAL BACKGROUND

The boundary layer is that part of the atmosphere where friction with, and heating by the surface play an important part in the generation of turbulence. Near the surface the turbulence properties can be scaled in terms of the Reynolds stress, τ_0 , and the surface sensible virtual temperature flux, Q_{0v} , using Monin-Obukhov similarity, where departures from neutral equilibrium are parameterized by Z/L . Those interested in a more complete treatment of the surface layer should refer to Businger (1973) and Wyngaard *et al.* (1971a and 1971b). The velocity and temperature are scaled by u_* and T_* and stability, L ,

$$\tau_0 = \rho u_*^2 \quad (3a)$$

$$Q_{0V} = -u_* T_{V*} \quad (3b)$$

$$L = \frac{T u_*^2}{\kappa g T_{V*}} \quad (3c)$$

where ρ is the density of air, T is the absolute temperature, T_V the virtual potential temperature, g the acceleration of gravity and κ is von Karmon's constant (we have used $\kappa = 0.35$). T_{V*} is related to the water vapor mixing ratio scaling parameter, q_* , by

$$T_{V*} = T_* + 6.1 \times 10^{-4} T q_* \quad (4)$$

where q is given in gm/kg.

In the inertial subrange of locally isotropic turbulence, fluctuations in horizontal wind speed and temperature can be characterized by a one-dimensional fourier power spectrum $S(k)$ (Tatarski, 1961)

$$S_u(k) = 0.52 \epsilon^{2/3} k^{-5/3} \quad (5a)$$

$$S_T(k) = 0.25 C_T^2 k^{-5/3} \quad (5b)$$

where k is the wavenumber, defined such that

$$\int_0^\infty S_x(k) dk = \langle (x - \bar{x})^2 \rangle \quad (6)$$

The values of various empirical constants (such as κ) were taken from Champagne et al. (1977).

In the surface layer, one can write expressions for ϵ (Wyngaard et al., 1971a) and C_T^2 (Wyngaard et al., 1971b)

THE BDM CORPORATION

$$\epsilon = \frac{u_*^3}{kZ} \phi_\epsilon (\xi) \quad (7a)$$

$$C_T^2 = T_*^2 Z^{-2/3} f(\xi) \quad (7b)$$

where $\xi = Z/L$. The present form of the dimensionless dissipation function, $\phi_\epsilon (\xi)$, is

$$\phi_\epsilon (\xi) = (1 + 0.5 |\xi|^{2/3})^{3/2} \quad \xi < 0 \quad (8a)$$

$$\phi_\epsilon (\xi) = (1 + 2.5 |\xi|^{2/3})^{3/2} \quad \xi > 0 \quad (8b)$$

while that for the dimensionless structure functions parameter, $f(\xi)$, is

$$f(\xi) = 4.9 (1 - 7\xi)^{-2/3} \quad \xi < 0 \quad (9a)$$

$$f(\xi) = 4.9 (1 + 2.4 \xi^{2/3}) \quad \xi > 0 \quad (9b)$$

The principle of similarity is invoked under the assumption that $|L|$ is considerably less than the height of the boundary layer, h . As was previously mentioned, this condition was not met for the stable data. Under unstable conditions the boundary layer height is determined by the height of the lowest inversion, Z_i (Deardorff, 1974), so that $h = Z_i$.

C. INSTRUMENTATION AND ANALYSIS

The platform for these measurements is a single engine turbo-charged Bellanca Viking operated by Airborne Research Associates. The aircraft is well instrumented allowing simultaneous measurements of air temperature, pressure, dew point, electric field, and infrared surface temperature. Details of the instrumentation and data acquisition are contained in a technical report (Fairall and Markson, 1979). We will only discuss several aspects of the turbulence measurements deemed relevant to the interpretation of the data.

THE BDM CORPORATION

Dissipation rate, ϵ , was determined from velocity fluctuations sensed with a constant temperature anemometer employing tungsten wires 4.5 μ in diameter and 1.7 mm in length operated at a 50% overheat. The signal was bandpass filtered ($f_l = 50$ Hz and $f_u = 500$ Hz) before being squared and averaged. One can calculate ϵ from the filtered mean square fluctuations using

$$\epsilon^{2/3} = \left(\frac{2\pi}{\bar{u}}\right)^{2/3} \frac{2}{3(0.52)} \frac{\langle(u - \bar{u})^2\rangle_{l,u}}{(f_l^{-2/3} - f_u^{-2/3})} \quad (10)$$

where $\bar{u} = 60$ m/sec is the average aircraft true airspeed.

Temperature structure function, C_T^2 , was determined from temperature difference fluctuations sensed with paired tungsten wires separated a distance $d = 0.85$ meters. Two complete systems were used (one ac wheatstone bridge and one dc) each employing an independent pair of wires. The two systems systematically disagreed by about 20%, possibly due to slightly different frequency response characteristics. The velocity sensitivity of the sensors as a function of bridge current was carefully measured at $\bar{u} = 60$ m/sec in the laboratory to optimize the temperature fluctuation measurements. The mean square temperature fluctuation data were corrected for velocity effects using the known velocity sensitivity and the values of velocity fluctuation intensity measured simultaneously with the hot-wire anemometer. Furthermore, one temperature bridge was operated at half the sensor current of the other in order to flag possible velocity sensitivity problems, should they occur. In practice, the velocity contribution to the temperature signal was considerably less than the system noise. C_T^2 was calculated using the equation

$$C_T^2 = \langle(T - \bar{T})^2\rangle_d d^{-2/3} \quad (11)$$

which is based on the assumption that the probe separation, d , is within the inertial subrange.

THE BDM CORPORATION

Because the larger scale eddies become more restricted as one approaches the sea surface, the measured values of C_T^2 and ϵ are subject to error due to the assumptions of isotropy in eqs. 10 and 11. This is particularly important for this data because of the unusually low altitudes ($Z = 3$ meters) employed. We have examined this question by replacing the inertial subrange forms of S_U and S_T with forms valid over the entire range of k . Thus, we can compute the actual measured values of the mean square fluctuations

$$\langle (u - \bar{u})^2 \rangle_{z,u} = \int_{f_\ell}^{f_u} S_U(f) df \quad (12a)$$

$$\langle (T - \bar{T})^2 \rangle_d = 2 \int_0^\infty [1 - \cos(kd)] S_T(k) dk \quad (12b)$$

where we have used the formulae for S_U and S_T given by Kaimal et al., (1972) for neutral stability. Since Kaimal et al., (1972) indicate that the size scales for unstable conditions are considerably larger than the neutral case, this calculation should serve to establish an upper limit on the effects. We have expressed the result in terms of the ratio of the measured to the actual value (ϵ_m/ϵ or C_{Tm}^2/C_T^2) as a function of altitude (Figure 2) for those filter frequencies and probe spacing used for the experiment. Based on this calculation, one can conclude that the surface effects on the measurements of ϵ were negligible and that the upper limit of the effects on the C_T^2 were on the order of 10%.

D. FLIGHT PATTERN

Aircraft are particularly useful for atmospheric research because they are able to sample large pieces of atmosphere in relatively short time periods. Unfortunately, even at sixty meters per second, one cannot expect to transverse the larger scale eddies normally associated with turbulence in just a few seconds. As a result, if one wishes to define the turbulence properties of the atmosphere to some reasonable statistical confidence, an averaging period of a few minutes (on the order of 10 kilometers) is required. Obviously for

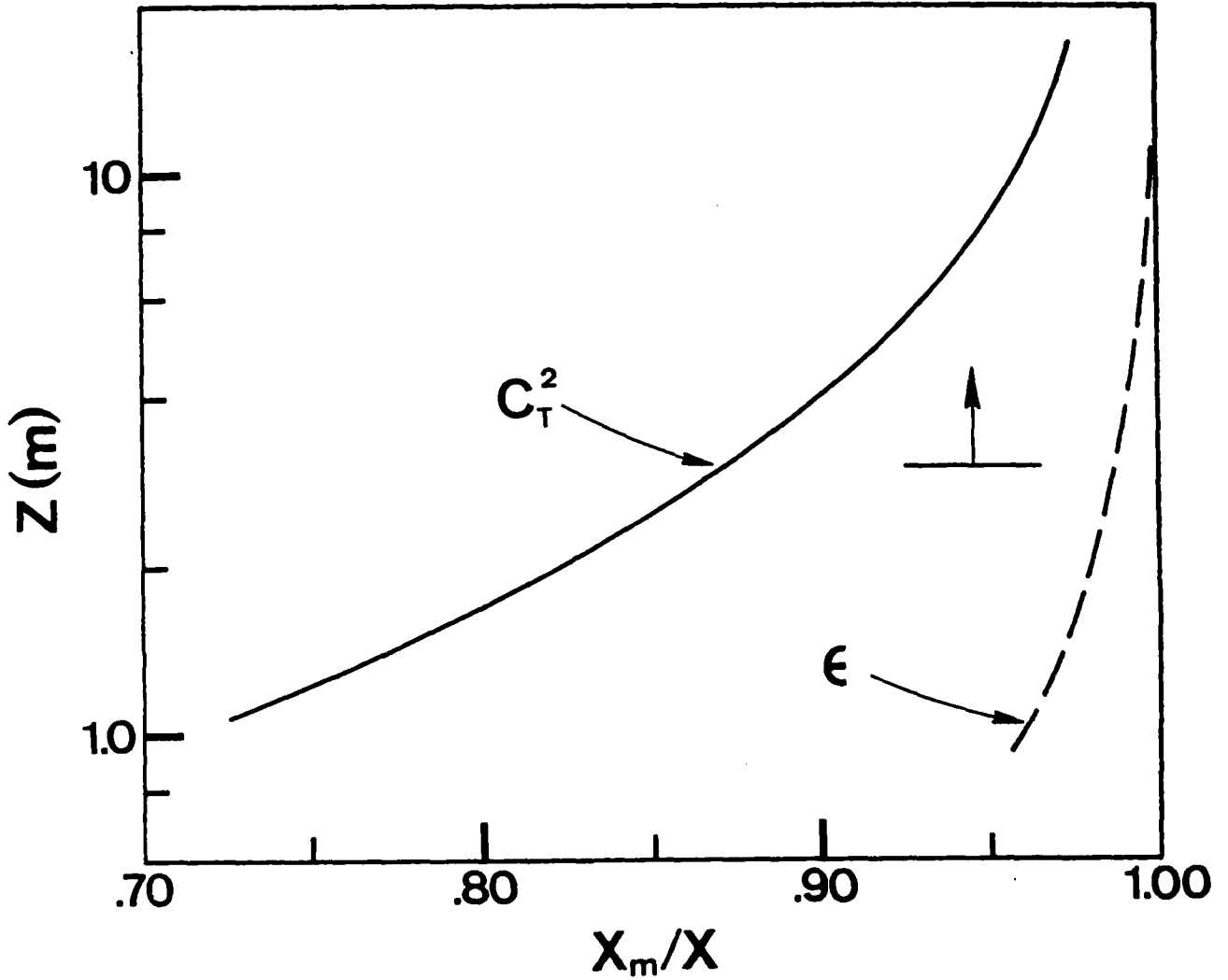


Figure 2. The Expected Effect of the Lower Isotropic Limit on the Turbulence Measurements as the Aircraft Nears the Sea Surface

The measurement error is expressed as the ratio of the measured value to the actual value (X_m/X) for (dashed line) and C_T^2 (solid line). The short horizontal line with the vertical arrow indicates the minimum altitude of the aircraft.

THE BDM CORPORATION

the surface layer investigation one not only requires very low altitude data but a greater density of measurement altitudes near the surface. The final flight pattern decided upon consists of a series of constant altitude runs of two minutes duration each at successively greater altitude. In order to maintain the same approximate location, the flight direction was reversed at alternate altitudes. Normally the process was started at the lowest altitude of three meters, as "eyeball" estimated by the pilot. At this point the aircraft altimeter was set to ten feet and subsequent altitudes were based on this setting. The altitudes of the level runs were increased approximately exponentially.

This type of flight pattern has been named a "ladder profile" with the two minute runs being the rungs of the ladder. The total time required to execute a complete ladder profile was on the order of 30 minutes.

E. SURFACE LAYER SCALING PARAMETERS

The Monin-Obukhov scaling parameters for each profile were obtained from the lowest two or three data points. First, q_* was calculated from a simple bulk formulation using a ten meter drag coefficient

$$q_* = 0.036 (q - q_s) \quad (13)$$

where q is the mixing ratio at $Z = 10$ meters and q_s is the value for the sea surface calculated from the sea surface temperature assuming 100% relative humidity. Given the relatively smaller contribution of q_* to L , a more sophisticated treatment of water vapor was not considered to be worthwhile. At this point, values of u_* and T_* were selected that gave good fits of eqs. 7a and 7b to the lower altitude values of ϵ and C_T^2 . Since $|\xi|$ was usually much less than unity in this region, the actual form of $\phi_\epsilon(\xi)$ and $f(\xi)$ would be de-emphasized in the determination of u_* , T_* , and L . The sign of T_* was determined from the air-sea temperature difference. The scaling parameters for all twenty-one profiles taken during PC II are given in Table 1.

THE BDM CORPORATION

TABLE 1. SURFACE LAYER SCALING PARAMETERS FOR THE LADDER PROFILES OBTAINED DURING PC II

N is the number of points in each profile; the other quantities are defined in the text.

Profile #	Date	Time	u_* (m/s)	T_* (°C)	q_* (gm/kg)	L (m)	h (m)	N
1	11/26	1252	0.400	-0.082	-0.160	-125	850	14
2	11/26	1436	0.230	-0.095	-0.160	- 50	900	14
3	12/02	1405	0.240	-0.135	-0.180	- 29	230	18
4	12/03	1108	0.290	0.030	0.000	233	200	11
5	12/03	1201	0.240	0.015	-0.018	420	60	10
6	12/03	1232	0.180	0.024	-0.009	120	60	9
7	12/03	1339	0.340	0.031	-0.040	403	120	11
8	12/05	1532	0.240	-0.260	-0.410	- 15	700	10
9	12/05	1624	0.260	-0.270	-0.400	- 16	700	13
10	12/07	1511	0.250	0.015	-0.007	390	75	12
11	12/07	1601	0.235	0.025	0.010	171	100	11
12	12/10	1259	0.530	-0.440	0.000	- 53	760	10
13	12/10	1324	0.380	-0.350	0.000	- 34	760	11
14	12/10	1410	0.320	-0.490	-0.490	- 15	760	15
15	12/10	1523	0.340	-0.480	-0.470	- 17	820	14
16	12/10	1637	0.340	-0.490	-0.500	- 16	980	14
17	12/11	1021	0.280	-0.440	-0.430	- 13	700	12
18	12/12	1642	0.280	-0.180	-0.500	- 24	800	18
19	12/13	1154	0.190	-0.210	-0.470	- 10	600	17
20	12.13	1459	0.170	-0.200	-0.420	- 9	550	14
21	12.13	1721	0.140	-0.120	-0.440	- 5	450	17

F. LADDER PROFILES

The locations of the profiles are indicated in Figure 3 by profile number. Profiles 12 and 13, which were overland, were not used in the results presented in Section 7. Since the profile data are completely cataloged elsewhere (Fairall and Markson, 1979), we will give only a few examples here. The situation encountered for the stable surface layers is illustrated in Figure 4 where the deviations of C_T^2 from the surface layer expression (eq. 7b) extend down to the lowest altitudes. The example given is one of the extremes. There were other stable profiles where the fit was much better, but, in general, the stable surface layers appeared to be dominated by the shallowness of the boundary layer.

The boundary layer was much more extensive on unstable days (the inversion height was typically 800 meters). In profile 1 (Figure 5a) the surface layer expression for C_T^2 is a good fit up to at least 300 meters. Note that in this case the upper altitude values of ϵ are smaller than expected based on the near surface values, while in profile 19 (Figure 5b) the reverse is true. This effect may be due to the fact that we ignored the possible existence of wind roll vortices (LeMone, 1973) or other two-dimensional structure. In Figure 5b the C_T^2 data displays a feature that often occurred. The higher altitude values are very well fit by a $Z^{-4/3}$ curve, but the actual values are not consistent with the near surface values, the near surface values of C_T^2 being somewhat lower than expected on the basis of the $Z^{-4/3}$ region. This aspect will be discussed in Section 7 and Section 8.

G. SURFACE LAYER DIMENSIONLESS TURBULENCE RESULTS

Given values of u_* and T_* for an unstable profile, the dimensionless quantities $\epsilon k Z/u_*^3$ and $C_T^2 Z^{2/3}/(4.9 T_*^2)$ were calculated for each data point. Because u_* and T_* were determined from the near surface values of ϵ and C_T^2 , the dimensionless quantities automatically have values near unity for $-Z/L \ll 1$. The dimensionless values were then averaged in bins of different dimensionless stability length allocated according to $\log|Z/L|$. Since

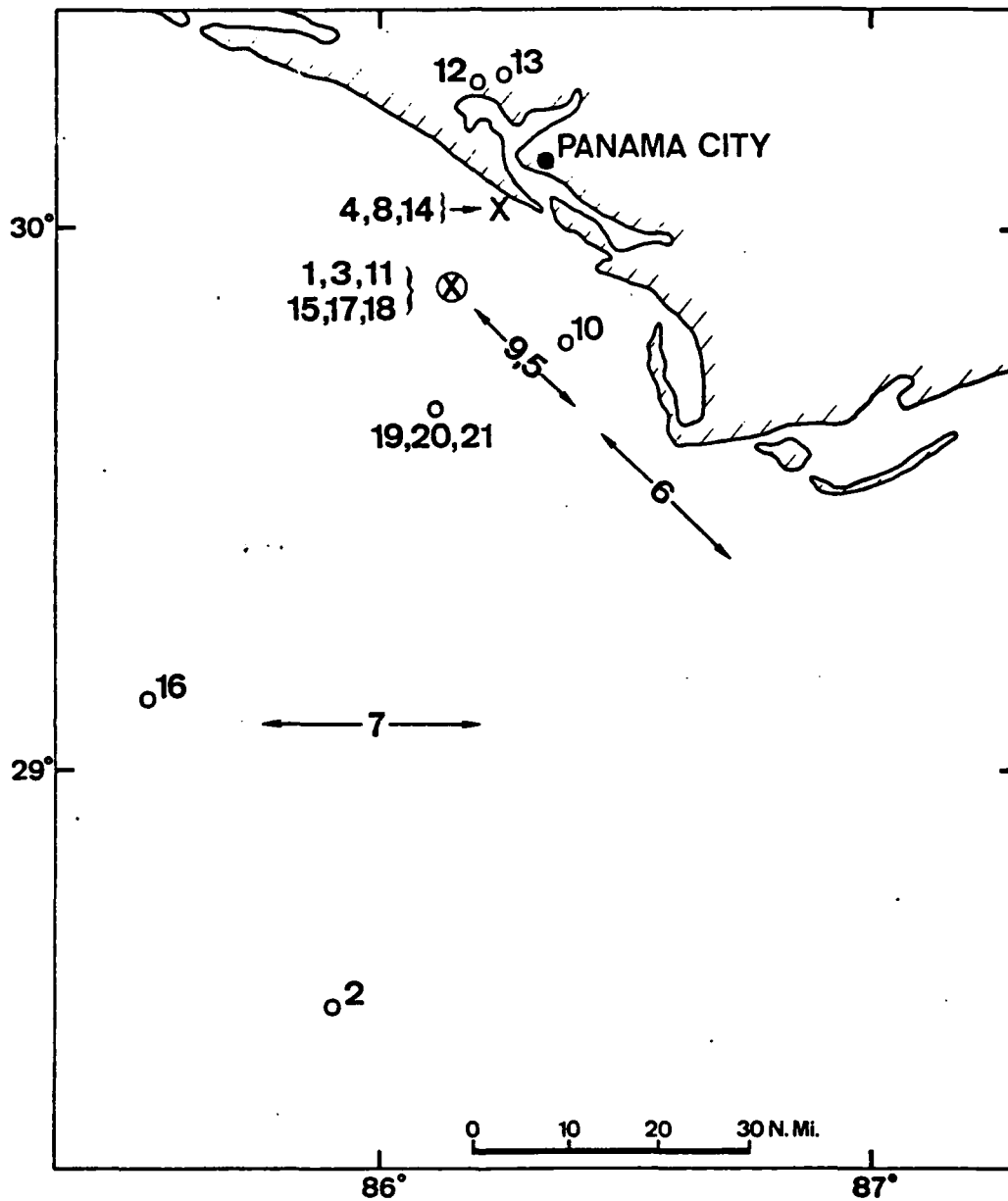


Figure 3. Locations of the Ladder Profiles in the Vicinity of Panama City, Florida

The circled X and X represent offshore platforms known as Stage I and Stage II, respectively. The numbers are the corresponding ladder profile designations.

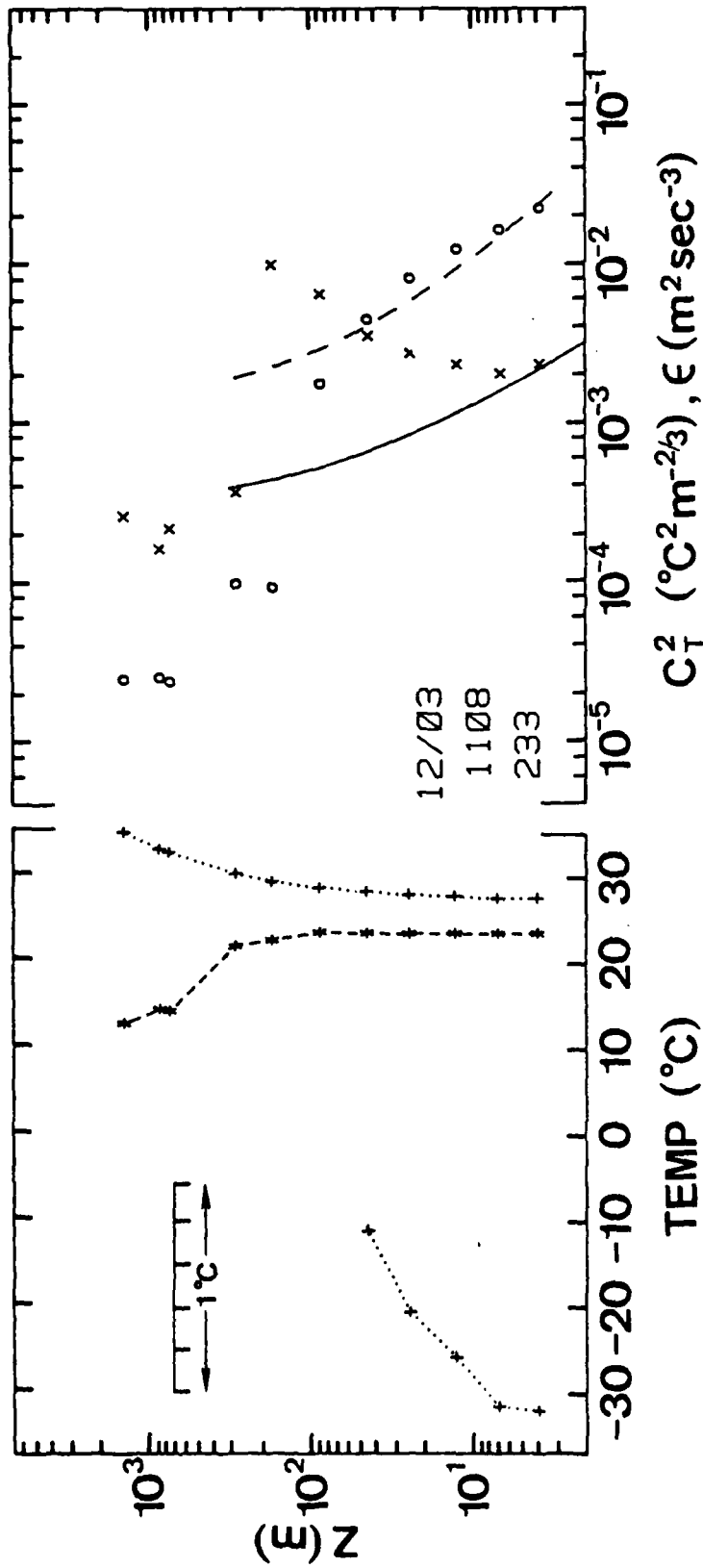


Figure 4. Ladder Profile #4

The data points plotted are virtual potential temperature (+), dew point temperature (*), C_{T2}^2 (x), and ϵ (o). The solid line is the MOS expression for C_T^2 and the long-dash line is the MOS expression for ϵ . The extreme left-hand side of the graph shows an expanded plot of virtual potential temperature.

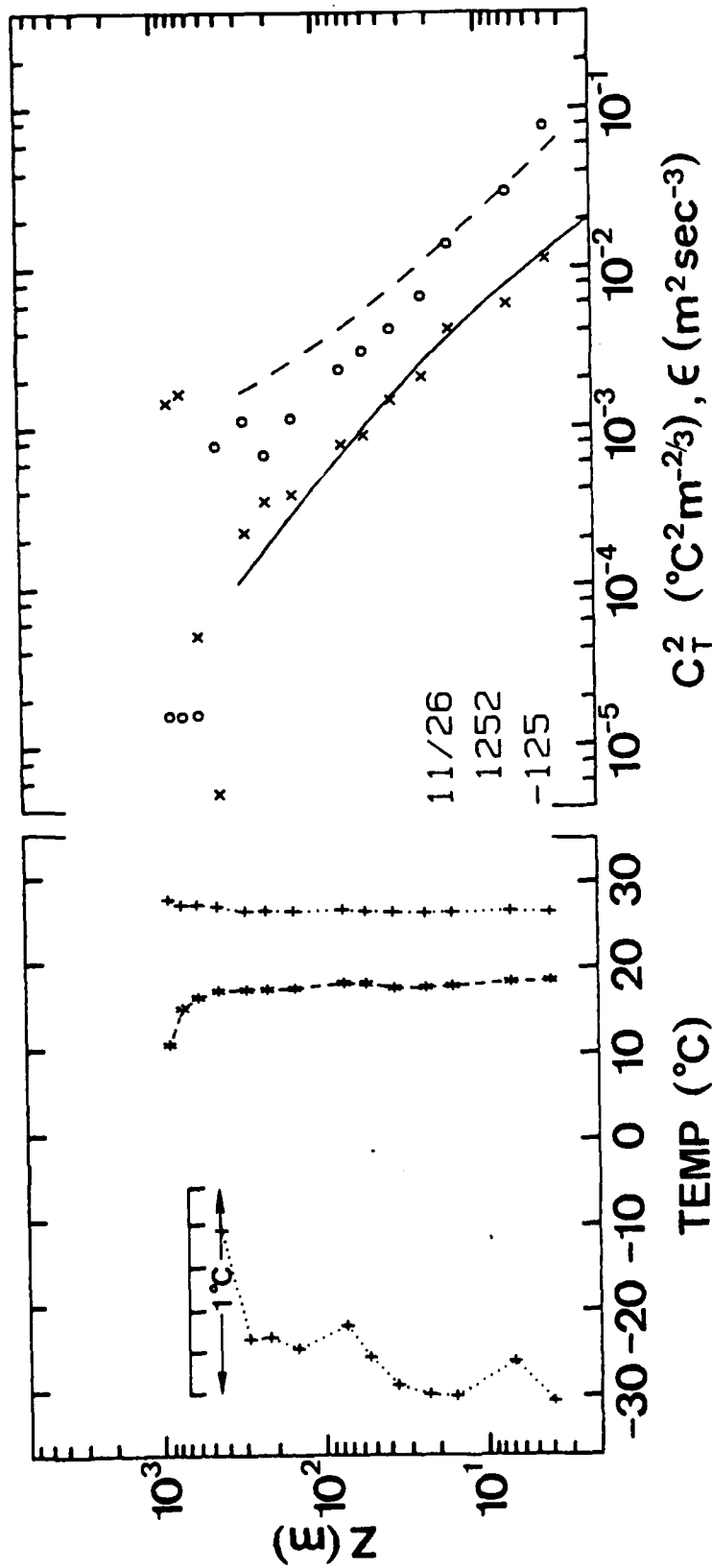


Figure 5a. Ladder Profile #1

The data points plotted are virtual potential temperature (+), dew point temperature (*), C_T^2 (x), and ϵ (o). The solid line is the MOS expression for C_T^2 and the long-dash line is the MOS expression for ϵ . The extreme left-hand side of the graph shows an expanded scale plot of virtual potential temperature.

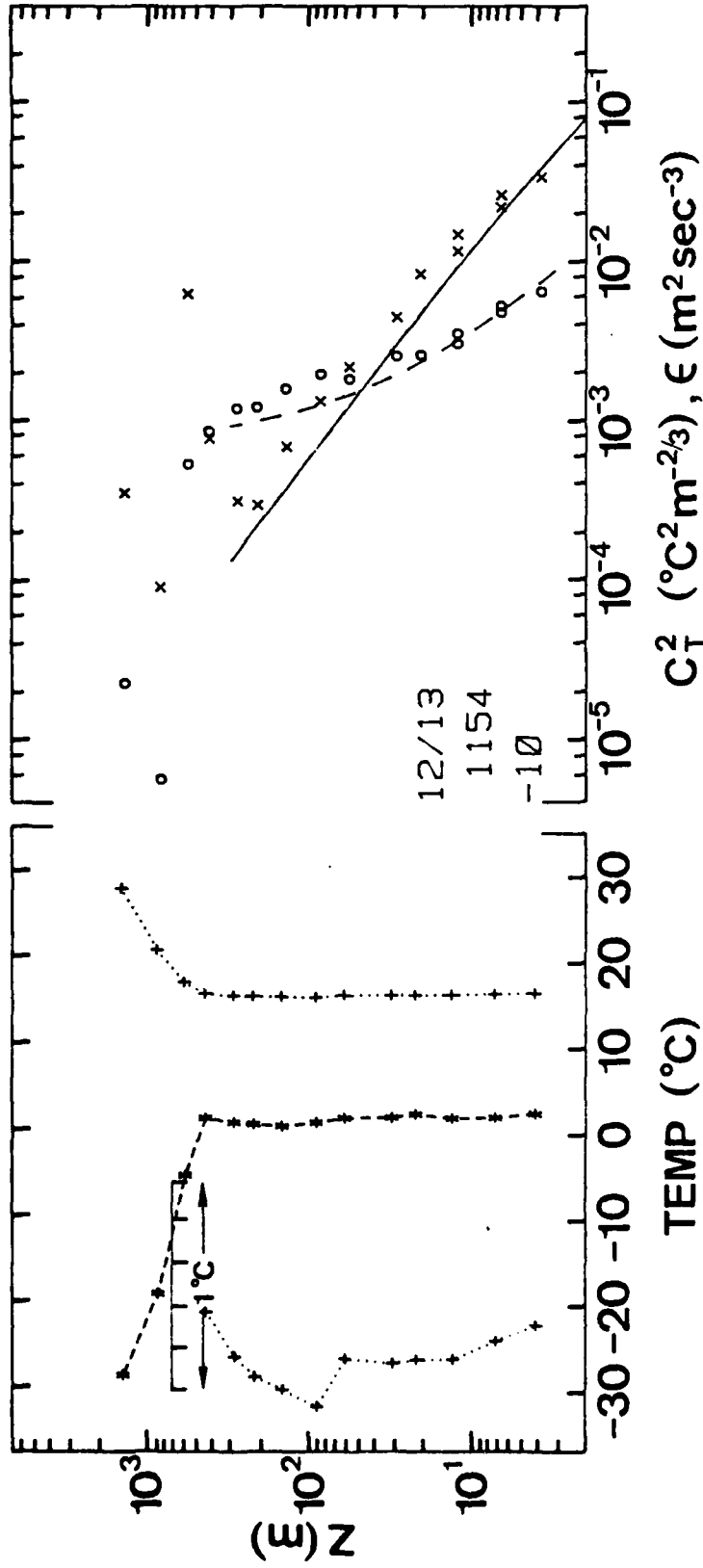


Figure 5b. Ladder Profile #19

The data points plotted are virtual potential temperature (+), dew point temperature (*), C_T^2 (x), and ϵ (o). The solid line is the MOS expression for C_T^2 and the long-dash line is the MOS expression for ϵ . The extreme left-hand side of the graph shows an expanded scale plot of virtual potential temperature.

THE BDM CORPORATION

the number of profiles taken on a given flight varied from one to five, a weighted average was used to avoid overemphasizing the conditions that happen to exist during those flights with more profiles. Each profile was assigned a weight $W = 1/M$ where M was the number of overwater profiles in that flight. In order to eliminate effects due to the inversion, the data had to be restricted based upon Z_i . The criteria that allowed the most data to be used without introducing inversion effects were

$$Z < Z_i - 100 \quad \text{for } \epsilon \quad (14a)$$

$$Z < 0.5 Z_i \quad \text{for } C_T^2 \quad (14b)$$

The results are given in Figures 6a and 6b with the solid curves representing eq. 8a and eq. 9a, respectively.

In order to examine the absolute height dependence (rather than the dimensionless height dependence) the quantity called R was calculated for each data point. R is the ratio of the dimensionless turbulence value to that value one would expect based on eq. 8a and 9a.

$$R_\epsilon = \frac{\epsilon k Z}{u_*^3} (1 + 0.5|Z/L|^{2/3})^{-3/2} \quad (15a)$$

$$R_T = \frac{C_T^2 Z^{2/3}}{4.9 T_*^2} (1 - 7 Z/L)^{2/3} \quad (15b)$$

The values of R were then averaged in bins of different altitude in a manner similar to that just described. The averages of R are shown in Figure 7, and the ratio of the standard deviation, σ_R , to R is shown in Figure 8. Taken together, these two figures illustrate one's ability to predict ϵ and C_T^2 as a function of height from near surface measurements. The 20% standard deviation for the near surface values (Figure 8) is due to the scatter inherent in the two minute averages.

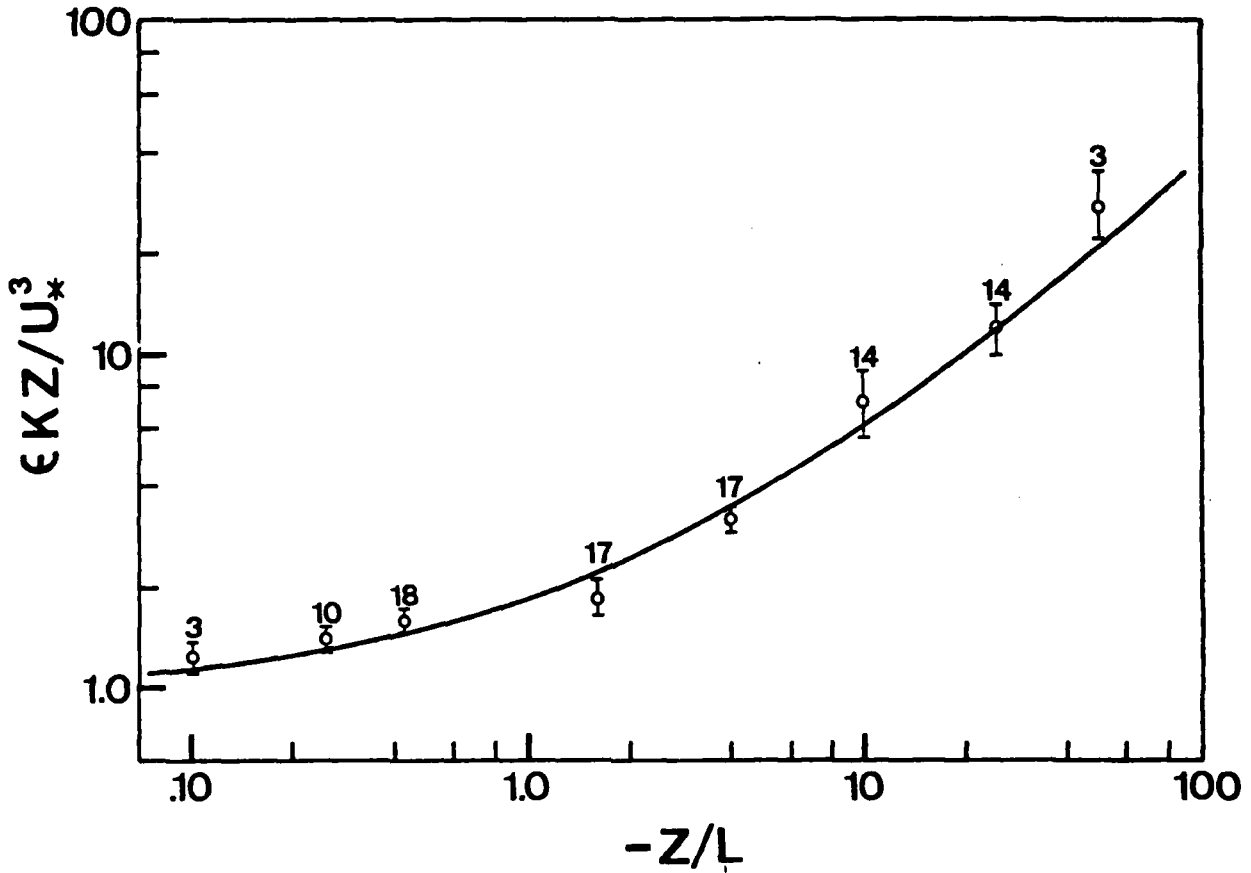


Figure 6a. Dimensionless Dissipation Rate as a Function of Dimensionless Atmospheric Stability

The points represent the weighted average of the profile data, the vertical bars represent the statistical error in the mean estimate, and the number is the weighted number of points in the average. The solid line is from eq. 8a.

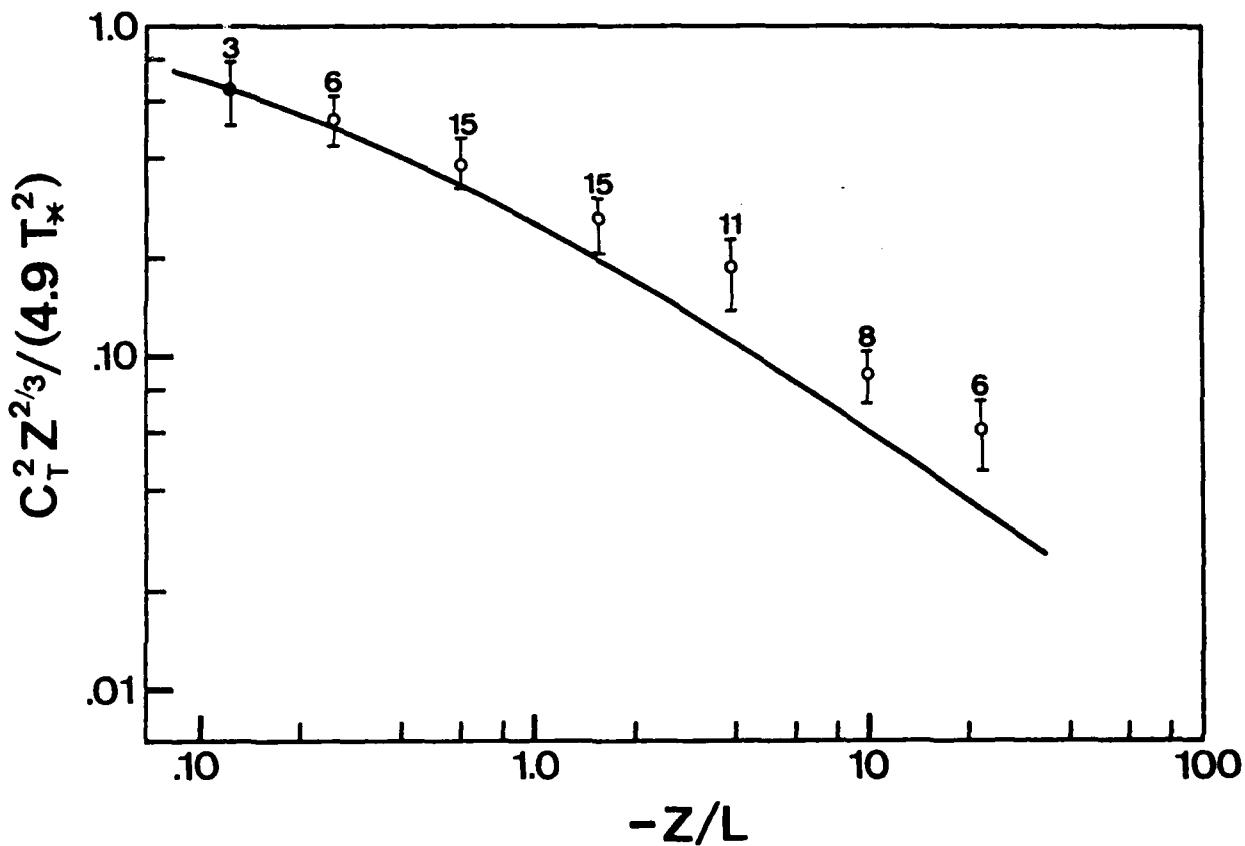


Figure 6b. Dimensionless Temperature Structure Function of Dimensionless Atmospheric Stability

The points represent the weighted average of the profile data, the vertical bars represent the statistical error in the mean estimate, and the number is the weighted number of points in the average. The solid line is from eq. 9a.

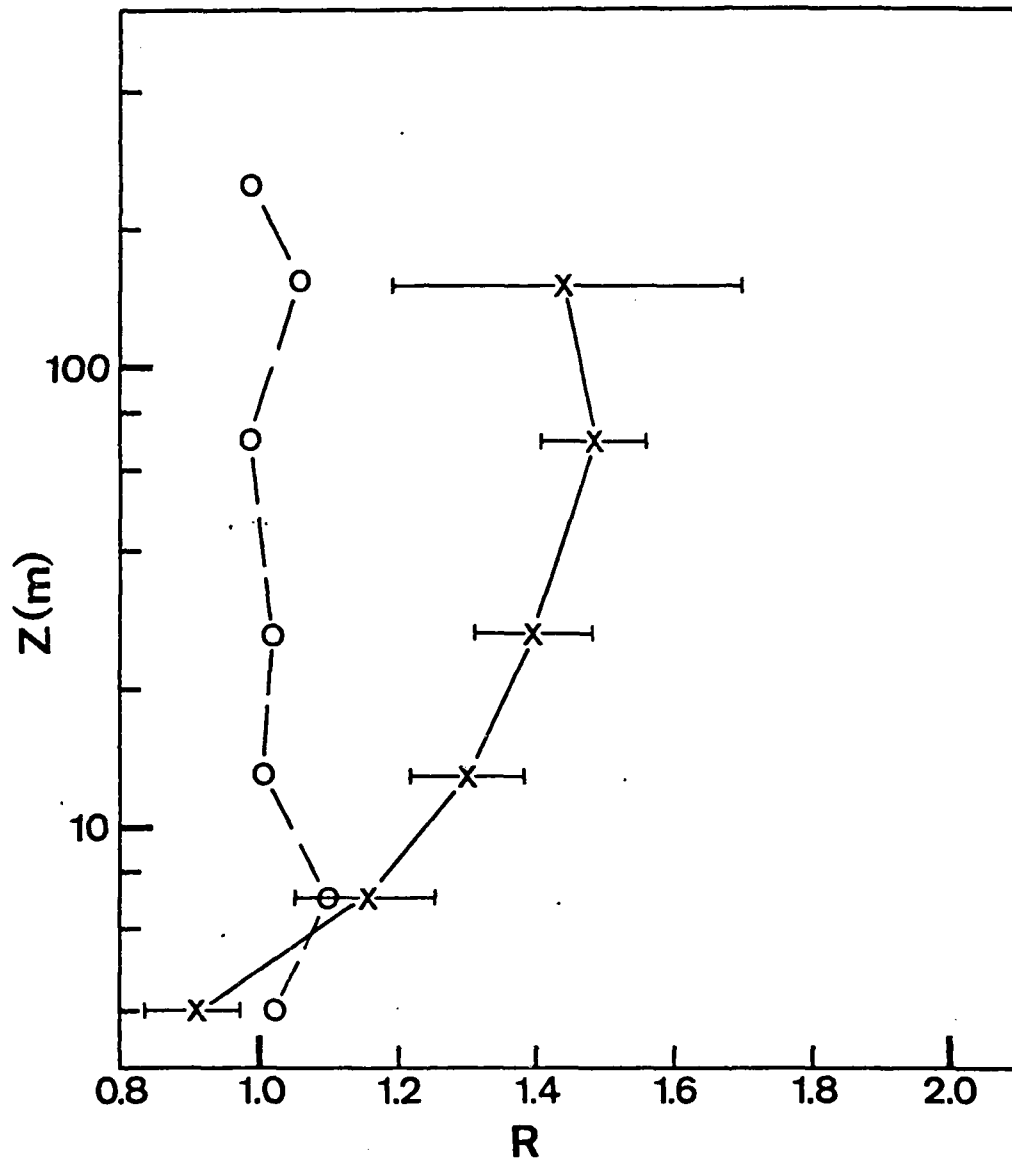


Figure 7. Weighted Average of R vs Altitude Where R is the Ratio of the Measured Value of the Turbulence Quantity to that Value Expected from Eq. 7a or Eq. 7b

The circles are for ϵ and the X's are for C_T^2 . The horizontal bars represent the errors in the mean estimate.

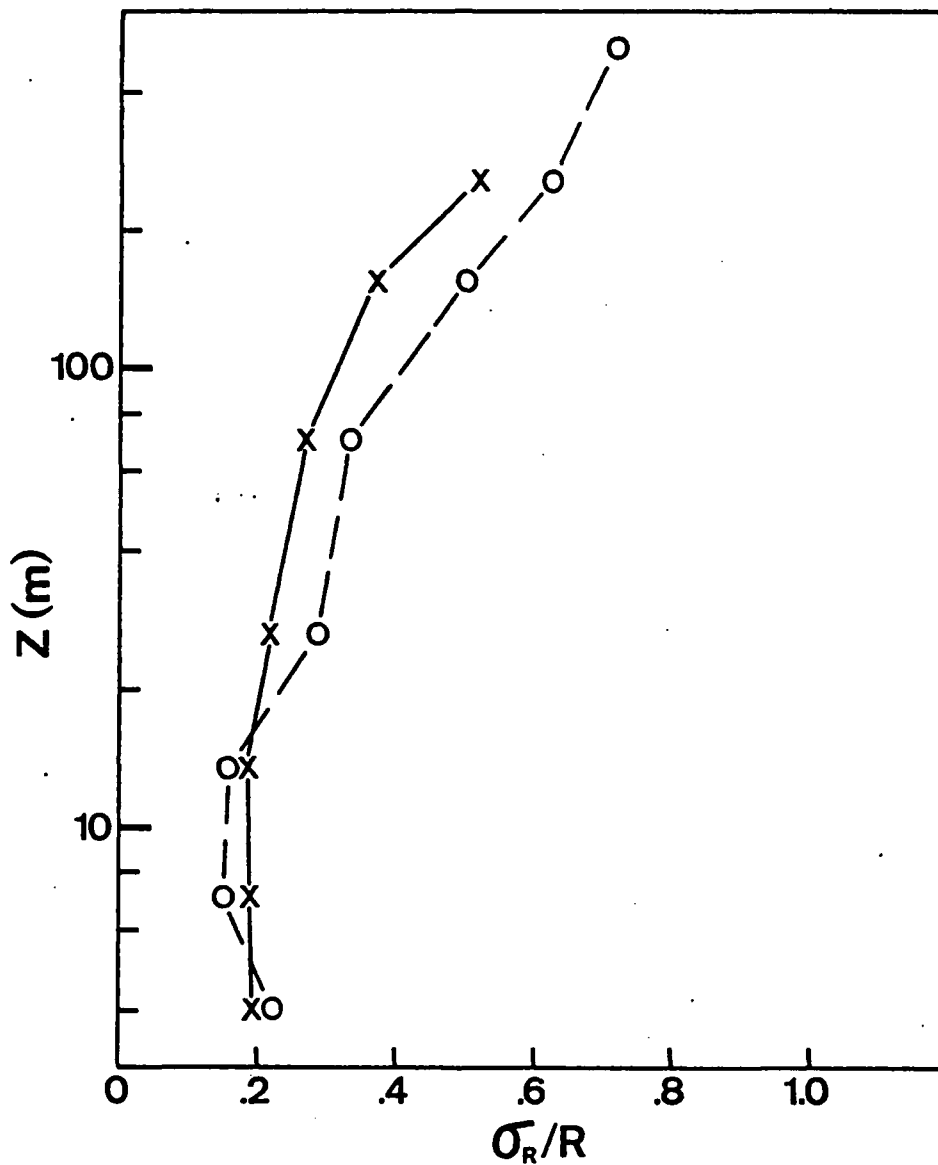


Figure 8. Fractional Random Error in Predictions of Turbulence Profiles Form Near Surface Measurements Using Eq. 8a and Eq. 9a

The circles are for ϵ and the X's are for C_T^2 .

H. DISCUSSION

Kaimal et al., (1976) divide the unstable boundary layer into three regions: the surface layer (Monin-Obukhov scaling), the free convection layer, and the mixed layer. Panofsky (1977) points out that the free convection layer is a region where Monin-Obukhov scaling and mixed layer scaling both apply. Hence, he has called this region the convective matching layer defined by $-L < Z < 0.1 Z_i$. At this point, we wish to consider how well the data fits the surface layer equations and the altitude limits of the fit.

Certainly the average fit of the ϵ data to eq. 8a (Figures 6a and 7) is surprisingly good. Furthermore, the formula gives reasonable results throughout the majority of the boundary layer ($Z < Z_i - 100$). The free convection limit of eq. 7a yields

$$\epsilon \rightarrow A (g/T) Q_{0V} \cdot -Z/L \gg 1 \quad (16)$$

where $A = 0.36$. Lenschow (1974) has found $A = 0.43$, while Kaimal et al., (1976) measured values of A between 0.5 and 0.7 overland. Actually, this limit was reached only on profile 21 which happened to be more consistent with $A = 0.5$.

In Figure 6b we can see considerable deviations of the C_T^2 from eq. 9a. The fact that the data lie on the expected curve for $-Z/L \ll 1$ is not significant since the values of T_* were selected to force a fit in this region. It is of interest to speculate on the possible significance of this disagreement. Recall that eq. 9a was based on overland measurements (Wyngaard et al., 1971b) with only a few points for $-Z/L > 1$. However, the more recent measurements of Kaimal et al., (1976) were examined in the convective limit of eq. 7a (note Q_0 is the sensible temperature flux, $-u_* T_*$)

$$C_T^2 = 2.67 (g/T)^{-2/3} Q_{0V}^{-2/3} Q_0^2 Z^{-4/3} \quad (17)$$

and excellent agreement was found for $0.1 Z_i < Z < 0.5 Z_i$. Thus, one can have confidence in eq. 9a for the overland case. The overwater measurements

of Davidson et al., (1979) show disagreement with eq. 9a similar to that of Figure 6b, but this disagreement is attributed to probable sea-salt contamination of the sensors. Frisch and Ochs (1975) found deviations in the $Z^{-4/3}$ height dependence of eq. 17 overwater for $Z > 0.1 Z_i$. However, they determined $Q_{OV}^{-2/3} Q_0^2$ from values of C_T^2 measured at $Z = 30$ m and did not look at lower altitudes. A corresponding analysis of the PC II data (determining $Q_{OV}^{-2/3} Q_0^2$ from the value of C_T^2 at $Z = 30$ m) shows no deviation from eq. 17 for $0.1 Z_i < Z < 0.5 Z_i$. The greater height dependence of R at lower altitudes (Figure 7) suggests that the discrepancy is some type of surface effect. Recall that in Section 3 the surface effect on the C_T^2 measurement process was estimated to have an upper limit of 10% at $Z = 3$ m (Figure 2). Certainly this does not preclude the possibility of some other measurement error such as frequency response losses or saturation effects, but at this writing no such effects have been discovered. Since we are unable to propose a physical mechanism for this discrepancy in the marine boundary layer, we prefer to leave this effect in the category of an interesting result. In the future, one of the C_T^2 systems will be operated with $d = 0.2$ m in the hope of resolving this dilemma.

REFERENCES

1. J. A. Businger, "Turbulent Transfer in the Atmospheric Surface Layer", Workshop on Micrometeorology, D. Haugen, Editor, American Meteorological Society, pp. 67-98 (1973).
2. F. H. Champagne, C. A. Friehe, J. C. LaRue, and J. C. Wyngaard, "Flux Measurements, Flux Estimation Techniques and Fine-Scale Turbulence Measurements in the Unstable Surface Layer Over Land", J. Atmos. Sci., 34, pp. 513-30 (1977).
3. K. L. Davidson, T. M. Houlihan, C. W. Fairall, and G. E. Schacher, "Observations of the Temperature Structure Function Parameter, C_T^2 , Over the Ocean", Bound.-Layer Meteor., 1979, to be published.
4. J. W. Deardorff, "Three Dimensional Numerical Study of the Height and Mean Structure of a Heated Planetary Boundary Layer", Bound.-Layer Meteor., 7, pp. 81-106 (1974).
5. C. W. Fairall and R. Markson, "Aircraft Measurements of Micrometeorological Parameters at Panama City, Florida in 1978", Naval Postgraduate School Technical Report, 1979. Copies can be obtained by writing to the authors or the Defense Documentation Center.
6. C. A. Friehe, J. C. LaRue, F. H. Champagne, C. H. Gibson, and G. F. Dreyer, "Effects of Temperature and Humidity Fluctuations on the Optical Refractive Index in the Marine Boundary Layer", J. Opt. Soc. Amer., 65, pp. 1502-11 (1975).
7. C. A. Friehe, "Estimation of the Refractive-Index Temperature Structure Parameter in the Atmospheric Boundary Layer Over the Ocean", Appl. Optics, 16, pp. 334-40 (1977).
8. A. S. Frisch and G. R. Ochs, "A Note on the Behavior of the Temperature Structure Parameter in a Convective Layer Capped by a Marine Inversion", J. Appl. Meteor., 14, pp. 415-9 (1975).
9. J. C. Kaimal, J. C. Wyngaard, Y. Izumi, and O. R. Cote, "Spectral Characteristics of Surface Layer Turbulence", Quart. J. Roy. Meteor. Soc., 98, pp. 563-89 (1972).
10. J. C. Kaimal, J. C. Wyngaard, D. A. Haugen, O. R. Cote, and Y. Izumi, "Turbulence Structure in the Convective Boundary Layer", J. Atmos. Sci., 33, pp. 2152-69 (1976).
11. M. A. LeMone, "The Structure and Dynamics of Horizontal Roll Vortices in the Planetary Boundary Layer", J. Atmos. Sci., 30, pp. 1077-91 (1973).

THE BDM CORPORATION

12. D. H. Lenschow, "Model of the Height Variation of the Turbulence Kinetic Energy Budget in the Unstable Planetary Boundary Layer", J. Atmos. Sci., 31, pp. 465-74 (1974).
13. H. A. Panofsky, "Matching in the Convective Planetary Boundary Layer", J. Atmos. Sci., 35, pp. 272-6 (1978).
14. V. L. Tatarski, Wave Propagation in a Turbulent Medium, McGraw-Hill, NY, 1961.
15. M. L. Wesley, "The Combined Effects of Temperature and Humidity Fluctuations on Refractive Index", J. Appl. Meteor., 15, pp. 43-9 (1976).
16. J. C. Wyngaard, O. R. Cote, and Y. Izumi, "Local Free Convection, Similarity, and the Budgets of Shear Stress and Heat Flux", J. Atmos. Sci., 28, pp. 1171-82 (1971a).
17. J. C. Wyngaard, Y. Izumi, and S. A. Collins, "Behavior of the Refractive Index Structure Parameter near the Ground", J. Opt. Soc. Am., 61, pp. 1646-50 (1971b).

THE BDM CORPORATION

INITIAL DISTRIBUTION LIST

	<u>DODAAD Code</u>	<u>No. of Copies</u>
1. Defense Documentation Center Cameron Station, Building 5 Alexandria, Virginia 22314	S47031	12
2. Library, Code 0212 Naval Postgraduate School Monterey, California 93940		2
3. Dean of Research, Code 012 Naval Postgraduate School Monterey, California 93940	N62271	1
4. C. W. Fairall, The BDM Corporation Naval Postgraduate School Monterey, California 93940		5
5. Professor K. E. Woehler, Code 61Wh Naval Postgraduate School Monterey, California 93940		1
6. Dr. Ralph Markson Airborne Research Associates 46 Kendal Common Road Weston, Massachusetts 02193		1
7. Assoc. Professor K. L. Davidson, Code 63Ds Naval Postgraduate School Monterey, California 93940		5
8. Assoc. Professor T. Houlihan, Code 69Hm Naval Postgraduate School Monterey, California 93940		1
9. Assoc. Professor G. Schacher, Code 61Sq Naval Postgraduate School Monterey, California 93940		5
10. Mr. Murray Schefer Code Air-3706 Naval Air Systems Command Washington, D.C. 20360		1
11. LT Michelle Hughes PM-22/PMS 405 Naval Sea Systems Command Washington, D.C. 20362		1

THE BDM CORPORATION

- | | | |
|-----|--|-------------|
| 12. | Dr. Stuart Gathman
Code 8326
Naval Research Laboratory
Washington, D.C. 20375 | 1 |
| 13. | Dr. Lothar Ruhnke
Code 8320
Naval Research Laboratory
Washington, D.C. 20375 | 1 |
| 14. | Dr. Barry Katz
Code 231
Naval Surface Weapons Center
White Oak Laboratory
Silver Spring, Maryland 20910 | 1 |
| 15. | Eugene J. Mack
Calspan Corporation
Buffalo, New York 14221 | 2 |
| 16. | Theodore V. Blanc
Code 8322B
Naval Research Laboratory
Washington, D.C. 20375 | 1 |
| 17. | Dr. J. H. Richter
Code 813
Submarine Systems Division
Communications Systems and Technology
Department
Naval Oceans Systems Center
San Diego, California 92152 | 1 |
| 18. | Jim Russell
D-910
Naval Avionics Center
6000 E. 21 Street
Indianapolis, Indiana 46218 | 1 |
| 19. | Dr. Andreas Gorocho
Naval Environmental Prediction Facility
Monterey, California 93940 | 1 |
| 20. | Dr. A. Weinstein
Director of Research
Naval Environmental Prediction Research Facility
Monterey, California 93940 | 1 |
| 21. | Dr. Phil Surra
Office of Naval Research | N62887
1 |

THE BDM CORPORATION

- | | | | |
|-----|---|--------|---|
| 22. | Director, Naval Research
Laboratory, Attn: Code 2627
Washington, D.C. 20375 | N00173 | 6 |
| 23. | Office of Naval Research
Branch Office
1030 East Green Street
Pasadena, California 91106 | N62879 | 1 |